

The Mechanism of Carbon Dioxide Adsorption in an Alkylamine-Functionalized Metal–Organic Framework

Nora Planas,^{†,‡} Allison L. Dzubak,^{†,‡} Roberta Poloni,^{‡,||} Li-Chiang Lin,[‡] Alison McManus,[†] Thomas M. McDonald,^{§,||} Jeffrey B. Neaton,[⊥] Jeffrey R. Long,^{§,||} Berend Smit,^{*,‡,§,||} and Laura Gagliardi^{*,†}

[†]Department of Chemistry, Supercomputing Institute, and Chemical Theory Center, University of Minnesota, Minneapolis, Minnesota 55455, United States

[‡]Department of Chemical and Biomolecular Engineering, University of California, Berkeley, California 94720, United States

[§]Department of Chemistry, University of California, Berkeley, California 94720, United States

^{||}Materials Sciences Division, Lawrence Berkeley National Laboratory, Berkeley, California 94720, United States

[⊥]Molecular Foundry, Lawrence Berkeley National Laboratory, Berkeley, California 94720, United States

Supporting Information

ABSTRACT: The mechanism of CO₂ adsorption in the amine-functionalized metal–organic framework mmen-Mg₂(dobpdc) (dobpdc⁴⁻ = 4,4'-dioxidobiphenyl-3,3'-dicarboxylate; mmen = *N,N'*-dimethylethylenediamine) was characterized by quantum-chemical calculations. The material was calculated to demonstrate 2:2 amine:CO₂ stoichiometry with a higher capacity and weaker CO₂ binding energy than for the 2:1 stoichiometry observed in most amine-functionalized adsorbents. We explain this behavior in the form of a hydrogen-bonded complex involving two carbamic acid moieties resulting from the adsorption of CO₂ onto the secondary amines.

The predicted growth of the global economy and world population in the near future will lead to an increased demand for energy,¹ resulting in even further increases in the concentration of CO₂ in the atmosphere. The development and worldwide utilization of efficient carbon capture and sequestration (CCS) technologies could reduce the CO₂ emissions associated with the use of fossil fuels.² Current carbon capture technologies generally use aqueous solutions of alkanolamines to scrub the flue gases.³ Amines are known to be very selective toward CO₂ capture from flue gases because of the strong chemical bonds formed in the chemisorption process. To overcome the energy penalty associated with the process, an important new development based on solid materials functionalized with amines has been proposed.^{4–10}

These materials have much lower heat capacities than aqueous amine solutions.¹¹ Of particular interest are amines grafted onto the open metal sites of metal–organic frameworks (MOFs). Indeed, recent experiments have shown that in the case of one particular MOF, Mg₂(dobpdc) (dobpdc⁴⁻ = 4,4'-dioxidobiphenyl-3,3'-dicarboxylate), *N,N'*-dimethylethylenediamine (mmen) can be bound to almost every open metal site lining the one-dimensional channels of the structure (Figure 1).⁴ The high adsorption enthalpy of mmen-Mg₂(dobpdc) for CO₂ endows the adsorbent with a significant capacity for CO₂ down to very low pressures.

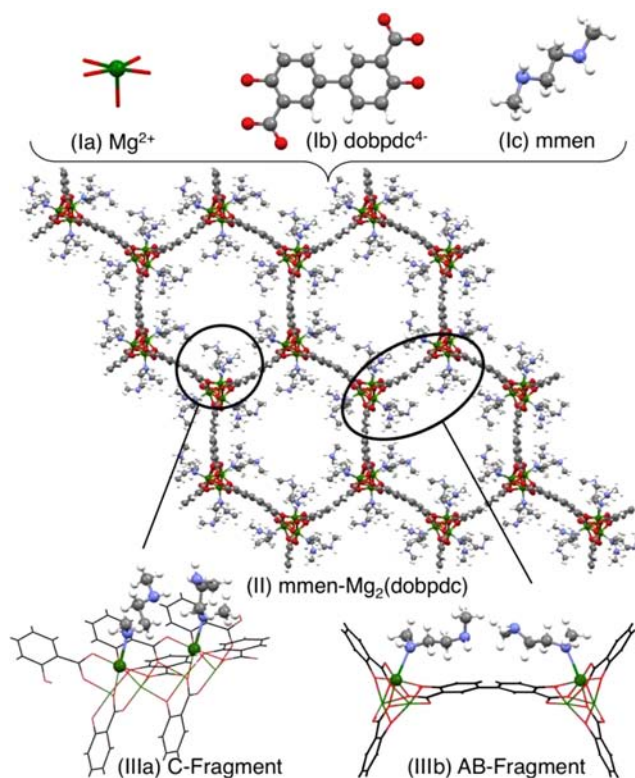


Figure 1. The mmen-Mg₂(dobpdc) structure used in this work. Color code: green, Mg; gray, C; blue, N; red, O; white, H. (Ia–c) Basic building blocks of mmen-Mg₂(dobpdc). (II) Minimum-energy configuration obtained from periodic density functional theory calculations, as shown from a view of the *ab*-plane cross section. (IIIa,b) The two fragments used as models in the calculations.

The regeneration energy of the solid adsorbent is lower than that of aqueous amine solutions because of its large working capacity and low heat capacity. Understanding reactivity

Received: January 15, 2013

Published: April 22, 2013

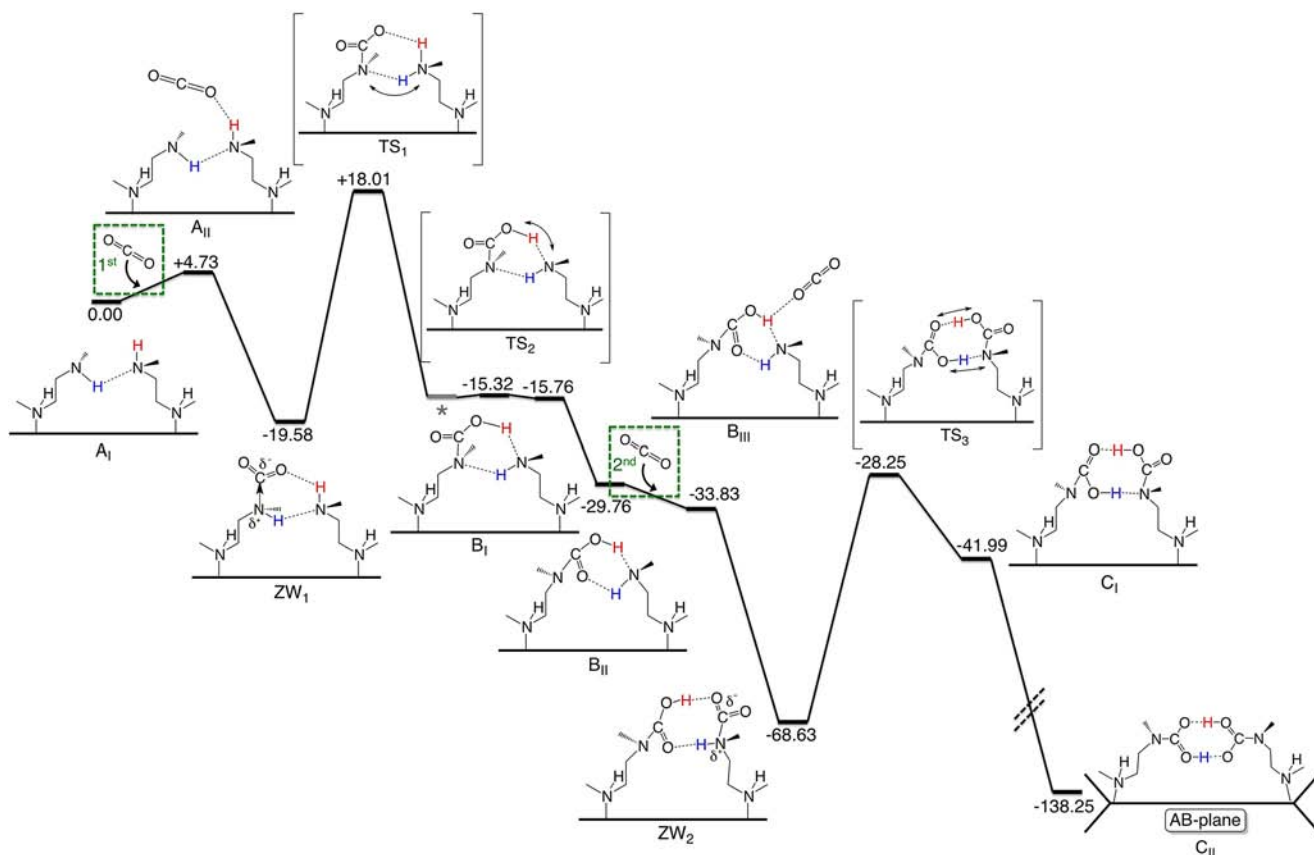


Figure 2. The proposed mechanism: (left) first CO₂ uptake (CO₂:amine = 1:2); (right) second CO₂ uptake (CO₂:amine = 2:2). The energy profile, ΔE , reported in kJ/(mol of model fragment), was calculated as $\Delta E = E_{\text{species}} - E_{A_1} - nE_{\text{CO}_2}$ where $n = 1$ (first uptake) or 2 (second uptake). The dashed diagonal lines indicate that the ΔE of species C_{II} is not drawn to scale. Coordinates and energies of all optimized species are given in sections 8–9 in the SI.

differences between solid and liquid adsorbents is essential for understanding the optimum reaction enthalpy for CO₂, thus informing the design of next-generation adsorbents with further reduced regeneration energies.

One would expect this material to capture CO₂ following conventional ammonium carbamate chemistry, in which the adsorption of each CO₂ requires two amines, one to participate in a nucleophilic attack on the carbon atom of CO₂ to form a C–N bond and the other to act as a base to abstract the proton. Interestingly, the isosteric heat of adsorption (Q_{st}) as a function of fractional coverage for mmen-Mg₂(dobpdc) shows that 0.8 mol of CO₂/mol of amine is strongly adsorbed [Figure S2 in the Supporting Information (SI) adapted from the experimental adsorption data of McDonald et al.⁴]. As it is unlikely that all of the amines are accessible to CO₂, these adsorption experiments suggest a 1:1 amine:CO₂ stoichiometry, indicating that only one amine is needed for every CO₂ molecule. This suggests that a different type of chemistry takes place in the material. Here we present the results of a quantum-chemical study that elucidates the reaction mechanism and explains the experimentally observed 1:1 stoichiometry for the CO₂ adsorption by amine molecules inside mmen-Mg₂(dobpdc). Our mechanism predicts the formation of a bis(carbamic acid) complex.

To date, aqueous alkanolamine solutions have been extensively studied and are still regarded as the state-of-the-art technology for CO₂ capture.³ Different mechanisms have been proposed for the reaction between CO₂ and amines,

depending on the nature of the amine and the reaction conditions.^{12–22} These are summarized in section 3 in the SI. In this work, we investigated the CO₂–amine reaction mechanism in mmen-Mg₂(dobpdc), for which the reaction medium is quite different compared with an aqueous environment. First, the experiments were carried out with pure CO₂ gas in the absence of water or any polar solvent. Second, the amine groups are fixed by the position of the metal centers within the structure, which is in turn imposed by the coordination of the linker to the metal centers. Finally, as mentioned previously, the experimental adsorption data of McDonald et al.⁴ indicate a 1:1 reaction stoichiometry instead of the conventional 2:1 stoichiometry (see section 2 of the SI for more detailed information).

To explore the reaction mechanisms, we identified two representative fragments to be used in this study. The C fragment allows for the consideration of interactions between nearest-neighbor amines along the crystallographic *c* axis (IIIa in Figure 1), and the AB fragment was considered in order to address the interactions between nearest neighbors across the organic linker (the “*ab* plane”) (IIIb in Figure 1). All of the computational details are reported in section 4 in the SI.

The starting point of our study is the minimum-energy configuration of the amines in the unreacted alkylamine-appended MOF mmen-Mg₂(dobpdc) (II in Figure 1). Our energy calculations show that the amines prefer to form hydrogen bonds along the *c* axis because the distance between the amines is sufficiently short (7.02 Å between the

corresponding metal centers) for this interaction to be energetically favorable. Interestingly, the structure resulting from hydrogen bonding of two amines across the linker in the AB fragment—where there is a distance of 12.96 Å between the corresponding metal centers—is higher in energy than the structure corresponding to the noninteracting amines. This is due to the fact that the hydrogen bond between amine groups only forms at the expense of lengthening the Mg–N distance, which imposes an energetically unfavorable penalty. The Mg–amine binding energy was found to be -135.6 kJ/mol; this is significantly greater than the Mg–CO₂ binding energy of -43.9 kJ/mol, which is consistent with the experimental heat of adsorption of CO₂ in Mg₂(dobpdc) in the absence of amines.⁴ Thus, the possibility of amine substitution by CO₂ coordination to the metal center can be discarded. Importantly, the Mg–OH₂ binding energy was found to be -82.66 kJ/mol, which indicates that the water molecules bound to 20% of the metal sites will not be displaced by CO₂ either. Hence, we did not account for their presence in the mechanism reported herein.

We propose the mechanism shown in Figure 2. Inspired by the termolecular mechanism,¹⁷ we propose a pathway in which all of the N–C bond formation steps are stabilized by the concerted breaking and forming of hydrogen-bonded adducts. These hydrogen bonds seem to play a critical role in avoiding the formation of formally charged reaction intermediates and products. As illustrated in Figure 2, the hydrogen-bonded lowest-energy diamine complex (A_I), which involves two nearest-neighbor amines along the *c* axis, initially forms a hydrogen bond between the noninteracting NH group (red H in A_I) and a CO₂ molecule, affording A_{II}. This interaction is required for the subsequent step, which yields a zwitterionic species stabilized by a hydrogen bond with a neighboring amine along the *c* axis (ZW₁). Subsequent proton exchange yields the carbamic acid represented in B_I. The B_I species, which is stabilized by two hydrogen bonds with the neighboring amine, then undergoes a reorganization that results in the more energetically favorable double hydrogen-bonding interaction shown in B_{II}.

Interestingly, in these systems we found that the conventional 2:1 chemistry does not lead to the most stable configuration. The addition of a second CO₂ molecule that forms a hydrogen bond with the carbamic acid–amine adduct (B_{II} to B_{III} in Figure 2) readily yields a second zwitterionic species, again stabilized by dual hydrogen bonds (ZW₂ in Figure 2). Subsequent proton exchange (to give C_I) followed by product reorganization yields a bis(carbamic acid) stabilized by double hydrogen bonding in a “head-to-tail” fashion in the final complex (C_{II}).

All of our attempts to compute the corresponding isolated (non-hydrogen-bonded) zwitterionic species or the more conventional ammonium carbamate complex converged to neutral products. Nonreacted amine and free CO₂ were obtained in the first case, and a carbamic acid hydrogen-bonded to the neighboring amine was computed in the second case.

In addition, we explored the possible role of the MOF linker as a base. The three different types of O atoms of the dobpdc⁴⁻ linker (Ib in Figure 1) were considered. In all cases, the proton initially bound to the O atom of the framework went back to the amine N atom during the optimization process, again yielding final species with no formal charge. Attempts to obtain analogous species with the AB fragment cluster calculation failed. In this configuration, the distance between the amines in

the *ab* direction imposed by the framework (12.96 Å across the ligand in the *ab* plane vs 7.02 Å along the *c* axis) is too long. This long distance frustrates the required hydrogen-bond formations for the different steps. However, the final bisacid head-to-tail conformation through the *ab* plane in C_{II} gives a more stable final product, since the CO₂ uptake results in lengthening of the chain of the appended amine-derived species.

The two consecutive CO₂ uptake processes start with the formation of a hydrogen bond between the CO₂ and an amine (A_I) or an amine-derived species (B_{II}). In each case, the optimization of the newly formed species (A_{II} or B_{III}, respectively), in which the hydrogen-bonded CO₂ molecule has been rotated to obtain a spatial arrangement in which its carbon atom is facing toward the nitrogen atom of the neighboring amine, smoothly converges into the corresponding zwitterionic species (ZW₁ or ZW₂). Thus, the formation of the zwitterions is highly exothermic (releasing ca. 25 kJ/mol for ZW₁ and ca. 35 kJ/mol for ZW₂), and barrierless transformations occur. The primary difference between the two consecutive paths for CO₂ uptake lies in the transition states from the corresponding zwitterions to the carbamic acid species. In the first case, the formation of B_I requires two consecutive transitions, the first (TS₁) involving proton transfer from the zwitterion nitrogen (blue H in Figure 2) to the amine and the second (TS₂) involving proton exchange from the protonated amine (red H in Figure 2) to the newly formed carbamate. In the second case, the two protons are exchanged in a concerted transition (TS₃). This transition is enabled by the quasi-planar spatial disposition of the carboxylic moieties involved. The energy barriers for these two transformations are ~ 40 kJ/mol, respectively. These barriers are of similar magnitude to those computed for alkanolamine reactions in solution as reported in the literature.¹⁵ The origin of the mechanistic differences between the two transitions results from the structural differences between the corresponding zwitterionic species (see Figure S6A,B).

Amine–CO₂ reactions in aqueous solution, where zwitterionic and charged species are stabilized by the polar medium, usually occur with a CO₂:amine stoichiometry of 1:2. Our calculations have revealed that in the absence of solvent, reactions that result in the formation of charged species are no longer possible because neither the neighboring amines nor the framework act as proton acceptors. This new reactivity does not stop at the 1:2 CO₂:amine stoichiometry but instead recruits an additional CO₂ molecule, resulting in 2:2 stoichiometry. For the proposed mechanism, we calculated an adsorption energy of -138.25 kJ per 2 moles of CO₂, which corresponds to an average adsorption energy of -69.13 kJ/mol. Our predicted adsorption energy is in good agreement with the experimental Q_{st} value of -71 kJ/mol.⁴

The mechanism revealed in this work shows that there is a requirement for some amine ordering preceding the CO₂ adsorption, which is consistent with the delay to reach the primary adsorption site (corresponding to C_{II}) observed in the adsorption isotherms. Since the adsorption of the first CO₂ molecule is exothermic and the energy barriers for the two CO₂ uptake events are of similar magnitude, once the first CO₂ molecule is adsorbed, the second CO₂ molecule adsorbs immediately to form ZW₂, which evolves to C_{II}. Hydrogen bonds formed along the *c* axis are crucial for the adsorption mechanism to proceed. In the last step, however, the mmn ligands, which are elongated by the adsorption of CO₂,

participate in more favorable hydrogen-bonding interactions across the linker. This reveals how crucial the length of the amine is for systems of this type, in which the structural constraints of the adsorbent govern the amine–amine interactions. The adsorption mechanism elucidated in this study is a clear example of the high potential of MOFs to exhibit new types of reactivity.

■ ASSOCIATED CONTENT

📄 Supporting Information

Computational details, computed structures and energies, discussions of experimental data, and a summary of previously reported mechanisms. This material is available free of charge via the Internet at <http://pubs.acs.org>.

■ AUTHOR INFORMATION

Corresponding Author

Berend-Smit@berkeley.edu; gagliard@umn.edu

Author Contributions

[#]N.P. and A.L.D. contributed equally.

Notes

The authors declare no competing financial interest.

■ ACKNOWLEDGMENTS

This research was supported by the U.S. Department of Energy under Contracts DE-FG02-11ER16283 (# SC0006860), DE-SC0001015, DE-AC02-05CH11231, and DE-FG02-12ER16362 (#SC0008688). (A detailed acknowledgement can be found in the SI.) A.L.D. is grateful for support through the Louise T. Dossall Fellowship. We thank Jeffrey Reimer, Xueqian Kong, and Christopher J. Cramer for useful discussions.

■ REFERENCES

- (1) *Climate Change 2007: The Physical Science Basis*; Solomon, S., Qin, D., Manning, M., Marquis, M., Averyt, K., Tignor, M. M. B., Miller, H. L., Jr., Chen, Z., Eds.; Contribution of Working Group I to the Fourth Assessment Report of the Intergovernmental Panel on Climate Change; Cambridge University Press: Cambridge, U.K., 2007.
- (2) Chu, S. *Science* **2009**, *325*, 1599.
- (3) Rochelle, G. T. *Science* **2009**, *325*, 1652.
- (4) McDonald, T. M.; Lee, W. R.; Mason, J. A.; Wiers, B. M.; Hong, C. S.; Long, J. R. *J. Am. Chem. Soc.* **2012**, *134*, 7056.
- (5) Demessence, A.; D'Alessandro, D. M.; Foo, M. L.; Long, J. R. *J. Am. Chem. Soc.* **2009**, *131*, 8784.
- (6) McDonald, T. M.; D'Alessandro, D. M.; Krishna, R.; Long, J. R. *Chem. Sci.* **2011**, *2*, 2022.
- (7) Danon, A.; Stair, P. C.; Weitz, E. J. *Phys. Chem. C.* **2011**, *115*, 11540.
- (8) Lu, W.; Sculley, J. P.; Yuan, D.; Krishna, R.; Wei, Z.; Zhou, H.-C. *Angew. Chem., Int. Ed.* **2012**, *51*, 7480.
- (9) Lu, W.; Sculley, J. P.; Yuan, D.; Krishna, R.; Zhou, H.-C. *J. Phys. Chem. C.* **2013**, *117*, 4057.
- (10) Das, A.; Choucair, M.; Southon, P. D.; Mason, J. A.; Zhao, M.; Kepert, C. J.; Harris, A. T.; D'Alessandro, D. M. *Microporous Mesoporous Mater.* **2013**, *174*, 74.
- (11) Mason, J. A.; Sumida, K.; Herm, Z. R.; Krishna, R.; Long, J. R. *Energy Environ. Sci.* **2011**, *4*, 3030.
- (12) Caplow, M. J. *Am. Chem. Soc.* **1968**, *90*, 6795.
- (13) Danckwerts, P. V. *Chem. Eng. Sci.* **1979**, *34*, 443.
- (14) Vaidya, P. D.; Kenig, E. Y. *Chem. Eng. Technol.* **2007**, *30*, 1467.
- (15) da Silva, E. F.; Svendsen, H. F. *Ind. Eng. Chem. Res.* **2004**, *43*, 3413.
- (16) Crooks, J. E.; Donnellan, J. P. *J. Chem. Soc., Perkin Trans. 2* **1989**, 331.

- (17) Vaidya, P. D.; Kenig, E. Y. *Chem. Eng. Technol.* **2010**, *33*, 1577.
- (18) Ramachandran, N.; Aboudheir, A.; Idem, R.; Tontiwachwuthikul, P. *Ind. Eng. Chem. Res.* **2006**, *45*, 2608.
- (19) Hartono, A.; da Silva, E. F.; Svendsen, H. F. *Chem. Eng. Sci.* **2009**, *64*, 3205.
- (20) Aboudheir, A.; Tontiwachwuthikul, P.; Chakma, A.; Idem, R. *Chem. Eng. Sci.* **2003**, *58*, 5195.
- (21) Hampe, E. M.; Rudkevich, D. M. *Chem. Commun.* **2002**, 1450.
- (22) Hampe, E. M.; Rudkevich, D. M. *Tetrahedron* **2003**, *59*, 9619.